

# Administration of 4-hexylresorcinol increases p53-mediated transcriptional activity in oral cancer cells with the p53 mutation

YEI-JIN KANG<sup>1</sup>, WON-GEUN YANG<sup>2</sup>, WEON-SIK CHAE<sup>2</sup>, DAE-WON KIM<sup>3</sup>,  
SEONG-GON KIM<sup>1</sup> and HORATIU ROTARU<sup>4</sup>

<sup>1</sup>Department of Oral and Maxillofacial Surgery, Gangneung-Wonju National University, Gangneung, Gangwon-do 25457;

<sup>2</sup>Daegu Center, Korea Basic Science Institute, Daegu 41566; <sup>3</sup>Department of Oral Biochemistry, College of Dentistry, Gangneung-Wonju National University, Gangneung, Gangwon-do 25457, Republic of Korea;

<sup>4</sup>Department of Cranio-Maxillofacial Surgery, 'Iuliu Hatieganu' University of Medicine and Pharmacy, Cluj-Napoca 400000, Romania

Received April 23, 2022; Accepted June 30, 2022

DOI: 10.3892/or.2022.8375

**Abstract.** The p53 mutation is inherent in over 50% of human cancers. In head and neck squamous cell carcinoma, the p53 mutation is associated with a poor prognosis. 4-Hexylresorcinol (4HR) is a pharmacologic chaperone. The present study aimed to investigate the effect of 4HR on p53 transcriptional activity in oral carcinoma cells with p53 mutations. To identify conformational changes induced by 4HR administration, peptides including the DNA-binding domain from mutant and wild-type p53 were synthesized, and Fourier transform infrared spectroscopy was performed. To determine the effect of 4HR on p53 mutant carcinoma cells, western blot analysis, p53 transcriptional activity analysis, MTT assay and apoptosis immunocytochemistry were performed. The YD-15 cell line has a mutation in the DNA binding domain of p53 (Glu258Ala). When p53 Ala-258 was coupled by 4HR, the p53 Ala-258 structure lost its original conformation and approached a conformation similar to that of p53 Glu-258. In the cell experiments, 4HR administration to p53 mutant cells increased p53 transcriptional activity and the expression levels of apoptosis-associated proteins such as B-cell lymphoma 2 (BCL2), BCL2-associated X (BAX) and BCL2-associated

agonist of cell death (BAD). Accordingly, 4HR administration on YD-15 cells decreased cell viability and increased apoptosis. In conclusion, 4HR is a potential substance for use in the recovery of loss-of-function in mutant p53 as a pharmacologic chaperone.

## Introduction

p53 is a tumour suppressor and is known as the 'Guardian of the Genome' (1). The function of p53 is the induction of apoptosis, regulation of cellular proliferation and DNA repair (2). As p53 is a transcription factor, its function will be dependent on its intranuclear transportation and its binding ability to the promoter region of target genes. p53 has 6 major domains: The N-terminal transactivation domain, activation domain 2, proline rich domain, DNA-binding domain, nuclear localization signalling domain and tetramerization domain (3). The activation of p53 is observed as a response to cytotoxic stress, such as DNA damage (4). Activated p53 is a tetramer with acetylation and phosphorylation that translocates into the nucleus (4-6). Then, p53 binds to the promoter of genes that transcribe genes associated with apoptosis or DNA damage repair (4).

The *TP53* mutation is a frequent finding in oral cancer (7,8). Several strategies against mutant *TP53* have been developed (8,9). The most frequent site of *TP53* mutation is the DNA-binding site (4). Mutant p53 may not bind properly to DNA, and its transcriptional activity will be lower than that of wild-type p53 (4,10). As a consequence, the expression level of genes associated with apoptosis is lowered, and their protein expression level is also decreased accordingly (4,8). Tumour cells can undergo uncontrolled cellular proliferation despite high levels of *TP53* or p53 expression (11). Certain types of mutant p53 can act as gain-of-function mutants (8,12). In this case, tumour invasion and angiogenesis can be accelerated with the help of mutant p53 (8,12). Mutant *TP53* can interact with other transcription factors that are responsible for invasive tumour growth (12). YD-15 cells are a mucoepidermoid carcinoma cell line in the oral cavity that has a mutation in *TP53* (13). The YD-15 cell has an amino acid change

---

*Correspondence to:* Professor Seong-Gon Kim, Department of Oral and Maxillofacial Surgery, Gangneung-Wonju National University, Jukheon-gil 7, Gangneung, Gangwon-do 25457, Republic of Korea  
E-mail: kimsg@gwnu.ac.kr

*Abbreviations:* 4HR, 4-hexylresorcinol; ROS, reactive oxygen species; HDAC, histone deacetylase; ER, endoplasmic reticulum; TGF- $\beta$ 1, transforming growth factor- $\beta$ 1; FBS, fetal bovine serum; DMSO, dimethyl sulfoxide; FT-IR, Fourier transform infrared; MTT assay, 3-(4,5-dimethylthiazol-2-yl)-2,5-diphenyltetrazolium bromide assay; OD, optical density; BAX, BCL2-associated X; BCL-2, B-cell lymphoma 2; BAD, BCL2-associated agonist of cell death

*Key words:* 4-hexylresorcinol, oral carcinoma, p53, apoptosis, pharmacologic chaperone

mutation in *TP53* from aspartic acid (hydrophilic) to alanine (hydrophobic) in the DNA binding domain (13). This amino acid change influences the DNA binding ability of p53. As a consequence, YD-15 cells do not undergo apoptosis despite a high level of p53 expression. YD-15 cells were selected for the study of mutant p53 function restoration.

A treatment strategy for carcinoma with the *TP53* mutation is restoring the p53 function (9). This strategy can be classified into the following three categories: i) targeting the degradation or direct inhibition of mutant p53; ii) binding to mutant p53 and inducing conformation change to a desirable form; and iii) targeting the viral enzymes that are responsible for the degradation of p53 (9). In particular, small molecules that can bind to mutant p53, inducing mutant p53 conformational changes, have been a specific focus in recent studies (9). PRIMA-1, APR-246 and CP-31398 are chemicals that can bind to p53, inducing mutant p53 conformational changes (9). Although these chemicals are interesting in terms of restoring mutant p53 conformation, they generate reactive oxygen species (ROS) by suppressing antioxidant enzymes (14). Although ROS may provide additional toxicity to cancer cells, ROS are also carcinogenic and toxic to normal cells (15). This is a limitation for the clinical application of these chemicals (14). Therefore, chemicals that can change mutant p53 conformation and have antioxidant properties should be investigated. 4-Hexylresorcinol (4HR) is a chemical chaperone that has antioxidant properties (16,17) and is an histone deacetylase (HDAC) inhibitor (18). The administration of 4HR induces endoplasmic reticulum (ER)-mediated stress potentially by protein folding changes (16). When 4HR is administered to HUVECs, the expression level of transforming growth factor- $\beta$ 1 (TGF- $\beta$ 1) is increased (19). This is a combined action of ER stress and HDAC inhibition (16,20). When 4HR is provided to microorganisms with mutant enzymes, the enzyme activity is recovered by 4HR administration (16). The administration of 4HR to KB cells shows an anticancer effect, but KB cells have wild-type p53 (21-23). Although 4HR administration has been shown to have anticancer effects in numerous types of cancer, the therapeutic effect of 4HR on cancers with *TP53* mutations has not been studied. 4HR may recover p53 DNA binding activity via its binding to mutant p53 and conformational change. This conformational change may restore p53-mediated apoptotic gene expression. In addition, HDAC inhibition by 4HR can increase the acetylation of p53. The acetylation of p53 is mainly found in its C-terminal domain and DNA-binding domain (3). The acetylation of p53 in the p53 DNA binding domain may neutralize its positive charge and improve its DNA binding ability. HDAC-mediated deacetylation of p53 strongly inhibits p53-dependent apoptosis (24). As a consequence, tumour cells with a *TP53* mutation may undergo apoptosis by 4HR administration. For the examination of mutant p53 conformational changes, the peptide sequence of the p53 DNA-binding domain from YD-15 cells was acquired and synthesized. The normal peptide sequence of the p53 DNA binding domain was used as a reference. The conformational changes before and after 4HR administration of the mutant peptide were examined by Fourier transform infrared (FT-IR) spectra. The 4HR administration capacity to improve the DNA binding ability of p53 was examined by a p53 transcription activity assay.

The induction of tumour cell apoptosis was evaluated by the examination of apoptosis markers and cytochrome *c* leakage. Additionally, the therapeutic effect of 4HR administration was also studied in an animal model.

## Materials and methods

**Cell culture.** YD-15 cells originated from the human tongue from patients with an initial diagnosis of mucoepidermoid carcinoma. YD-15 Bank (accession no.: CVCL\_8930) and YD-9 (accession no. CVCL\_L080) cells were purchased from the Korean Cell Line Bank. The subsequent culture conditions were in accordance with those recommended by the Korean Cell Line Bank. Cells were cultured in six-well culture plates in a humidified 5% CO<sub>2</sub> incubator at 37°C. The freezing media were 52.5% Roswell Park Memorial Institute-1640 (RPMI-1640) medium supplemented with 40% fetal bovine serum (FBS) and 7.5% dimethyl sulfoxide (DMSO; all from Thermo Fisher Scientific, Inc.). Culture media were composed 90% by RPMI-1640 with L-glutamine (300 mg/l), 25 mM HEPES and 25 mM NaHCO<sub>3</sub>, and 10% by heat-inactivated FBS. Two-thirds of the medium was removed and replaced with fresh medium every 3 days.

**Peptide synthesis.** Two kinds of artificial peptides were designed from normal and mutant p53 of YD-15 cells. Glutamic acid at the 258th amino acid in p53 was replaced by alanine in YD-15 cells (13). The DNA-binding domain of p53 was from amino acids 102 to 292. Accordingly, mutation in YD-15 cells was localized in the p53 DNA binding domain (13). The artificial peptides were fabricated by Peptron. The amino acid sequences were ILTIITL-[E]-DSSGNLLGRNSF and ILTIITL-[A]-DSSGNLLGRNSF in the peptide from wild-type p53 and mutant p53 of YD-15 cells, respectively.

**FT-IR spectroscopy.** 4HR (cat. no. 209495) was purchased from Sigma-Aldrich; Merck KGaA. A sample was prepared as a mixture with 0.1% ethanol, and the concentrations were p53 Glu-258 (1 mg/ml), p53 Ala-258 (1 mg/ml), and p53 Ala-258 (1 mg/ml) + 4HR (0.1 mg/ml). FT-IR absorption spectra were obtained using a Fourier transform spectrometer (Vertex 80; Bruker Corporation) equipped with an attenuated total reflectance accessory (MIRacle; PIKE Technologies). The spectra were recorded in the spectral range of 600 to 4,000 cm<sup>-1</sup> at a resolution of 4 cm<sup>-1</sup> with a deuterated L-alanine-doped triglycine sulfate detector, and 128 repeated scans were averaged for each spectrum.

**Western blot analysis.** 4HR was solubilized in 0.1% DMSO. When YD-15 and YD-9 cells were cultured to ~70% confluence, they were treated with 1, 10 and 100  $\mu$ M 4HR for 2, 8, or 24 h; control cells were treated with 0.1% DMSO in culture medium. Cultured cells were treated with 0.01% trypsin and 1 mM ethylene-diamine-tetra-acetic acid. Then, they were harvested with a spatula. Cellular lysis was carried out with protein lysis buffer (PRO-PREP™; Intron Biotechnology, Inc.). The protein quantification was performed by Bradford method as previously described (19). The type of gel used was 15% SDS-polyacrylamide gel. The amount of protein loaded per lane was 30  $\mu$ g. The type of membrane used was

polyvinylidene difluoride (cat. no. IPVH00010; Millipore). The membrane was blocked with TBS-T (25 mM Tris-HCl, 140 mM NaCl, 0.1% Tween-20, pH 7.5) buffer containing 5% non-fat dry milk for 1 h at room temperature. Collected lysates underwent western blotting for B-cell lymphoma 2 (BCL2), BCL2 associated X (BAX) and BCL2 associated agonist of cell death (BAD). Antibodies against BCL2 (cat. no.: sc-7382), BAX (cat. no. sc-7480), BAD (cat. no. sc-8044) and  $\beta$ -actin (cat. no. sc-8432) were purchased from Santa Cruz Biotechnology, Inc. Dilution ratio was 1:1,000. The primary antibodies were incubated at 4°C overnight. The secondary antibodies used were HRP-conjugated (cat. nos. sc-2357 and sc-516102, Santa Cruz Biotechnology, Inc.) and its dilution ratio was 1:1,000. To detect HRP-labelled antibodies, Immobilon Forte Western HRP substrate (cat. no. WBLUF0500; MilliporeSigma) was used as chemiluminescence reagent. Blots were imaged and quantified using a ChemiDoc XRS system and Image Lab 3.0 (both from Bio-Rad Laboratories, Inc.).

*p53 transcriptional activity.* The p53 transcription factor assay was performed using a p53 transcription factor assay kit (cat. no. ab207225; Abcam). All antibodies used for the assay were included in the kit. For the quantitative measurement of p53 activation in human nuclear extracts, a specific single-stranded DNA containing the p53 DNA-binding site (5'-GGACAT GCCCGGGCATGTCC-3') was immobilized onto a 96-well plate. Active p53 present in the nuclear extract specifically binds to the oligonucleotide. p53 was detected by a primary antibody that recognizes an epitope of p53 accessible only when the protein is activated and bound to its target DNA. An HRP-conjugated secondary antibody provided a sensitive colorimetric measurement at optical density (OD) of 450 nm. To assess the effect of 4HR administration on the binding of mutant p53 to the consensus DNA sequence, 1, 10, and 100  $\mu$ M 4HR were applied, and nuclear extracts were collected after 2 h. The subsequent procedures were performed in accordance with the manufacturer's protocol. Briefly, samples were added to the appropriate wells and the plate was incubated for 1 h at room temperature with mild agitation. After washing each well three times with 200  $\mu$ l of 1X washing buffer, primary antibody was added to the wells. After covering the plate, it was incubated again for 1 h at room temperature without agitation. After the washing process, an anti-rabbit HRP-conjugated secondary antibody was applied and its dilution ratio was 1:1,000. The plate was incubated for 1 h at room temperature without agitation. After another washing process, a developing solution was added, and the plate was incubated for 5 min. Then, a stop solution was added, and the absorbance was measured at 450 nm.

*3-(4,5-Dimethylthiazol-2-yl)-2,5-diphenyltetrazolium bromide (MTT) assay.* MTT assays were conducted as follows: YD-15 cells were cultured as aforementioned. When YD-15 cells were cultured to ~70% confluence, they were treated with 1, 10 and 100  $\mu$ M 4HR for 24 or 48 h, and control cells were treated with 0.1% DMSO in culture medium. Then, the cells were incubated with yellow tetrazolium salt and 3-(4,5-dimethylthiazole-2-yl)-2,5-diphenyltetrazolium bromide (MTT) solution (Cell Proliferation kit I; Roche Molecular Diagnostics) for 4 h

at ambient temperature. Formazan crystals were solubilized with DMSO overnight, and the products were quantified spectrophotometrically by measuring the absorbance at 590 nm using a Victor Multilabel Counter (PerkinElmer, Inc.).

*Confocal microscopic examination.* When YD-15 cells were cultured on chamber slides at ~70% confluence, they were treated with 1, 10, and 100  $\mu$ M 4HR for 24 h. After fixation using 4% formaldehyde (diluted in PBS) at 4°C for overnight, the slides were washed with PBS with Tween-20. Then, protein blocking was performed with a blocking reagent (cat. no. X0909; Dako; Agilent Technologies, Inc.) for 30 min at room temperature. The cytochrome *c* apoptosis ICC Antibody kit (cat. no. ab110417; Abcam) was composed of a cytochrome *c* monoclonal antibody and ATP synthase V subunit  $\alpha$  monoclonal antibody. Cytochrome *c* and ATP synthase V are localized in the mitochondria, and only cytochrome *c* is released from mitochondria during apoptosis (25). As anti-cytochrome *c* antibody was conjugated with FITC and anti-ATP synthase V antibody with TxRd, the cells with cytochrome *c* leakage showed green fluorescence only. Pre-treated and fixed YD-15 cells were incubated with anti-cytochrome *c* antibody and anti-ATP synthase V antibody in a humidified dark chamber for 1 h. The nuclei were counterstained with 5 mg/ml DAPI at room temperature for 5 min. After washing, each slide was mounted. The mounted slides were examined with Stellaris 5 (Leica Microsystems GmbH) at the Center for Scientific Instruments, Gangneung-Wonju National University.

*Xenograft study.* The animal study was approved (approval no. GWNU-2021-3, approval date 2021.01.15) by the Animal Care and Use Guidelines of the College of Dentistry at Gangneung-Wonju National University (Gangneung, Republic of Korea). The approved duration of the experiment was a year. A total of 20 athymic male nude mice (7 weeks-old, body weight: 21~23.5 g) were approved for the present study and were introduced from ORIENT BIO, Inc. After receiving the animals, the adaptation period was allowed for 5 days. The light/dark cycle was 12/12 h. Mice were kept in individual cage with *ad libitum* access to food and water. The cage used was filter-bonneted individually ventilated cage. Food was sterilized and water was acidified to pH 2.5-3.0. The temperature in the specialized husbandry was set at 23-27°C. Cages were changed under a laminar flow hood. The number of injected YD-15 cells for each animal was ~3x10<sup>5</sup> cells. The resuspension solution was the culture media used for cell culture. They were injected into the sublingual space through the skin under anaesthetic conditions. Anaesthesia was induced by inhalation of 3% isoflurane. After injection, tumour growth was observed daily. In cases of successful tumour formation, the animals were included in the treatment groups. The nude mice showing evident tumour formation were randomly assigned to two groups: the 4HR and control groups. After the first injection, 12 mice showed tumour formation (Fig. S1). One mouse died. The same number of mice was assigned to each group. The second tumour injection was performed for the remaining 7 mice. Another 4 mice showed tumour formation, and the remaining 3 mice did not show any tumours. A total of 16 mice were included for drug administration. As the mice in the control group showed early loss during observation among the first 12 mice, 9 mice were assigned to

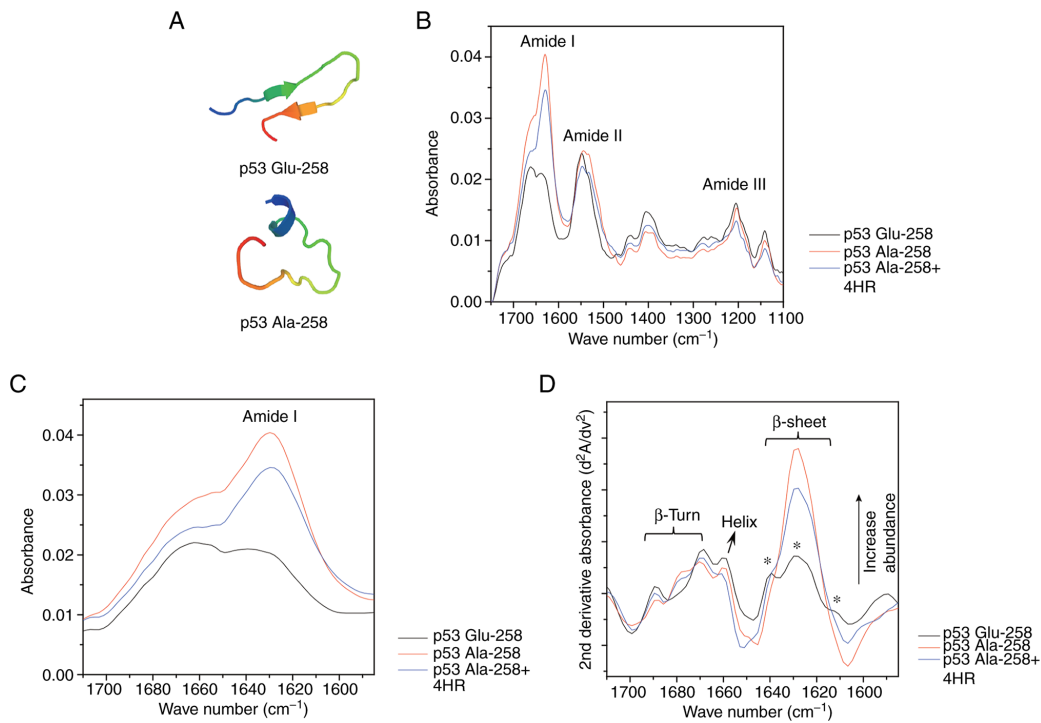


Figure 1. Conformational change of the peptide from mutant p53 by 4HR. (A) According to amino acid sequence-based peptide conformation prediction, the peptide from mutant p53 (p53-Ala-258) has a random coil structure, but the peptide from wild-type p53 has a beta-sheet structure (p53-Glu-258). (B) The Fourier transform infrared spectrum of each peptide showed a series of absorption bands at 1,600-1,700 (amide I), 1,480-1,580 (amide II) and 1,230-1,300 cm<sup>-1</sup> (amide III). (C) The amide I peak (C=O stretching) of p53-Ala-258 + 4HR was less enhanced than that of p53-Ala. (D) p53-Glu-258 showed rich β-sheet conformations detectable at 1,614, 1,628, and 1,639 cm<sup>-1</sup> (\*), whereas p53 Ala-258 showed a simple conformation mostly detected at 1,628 cm<sup>-1</sup>. When p53 Ala-258 was coupled by 4HR, it lost its original conformation and resembled the conformation of p53 Glu-258. 4HR, 4-Hexylresorcinol.

the control group, and 7 mice were assigned to the 4HR group. The drug was injected into the back subcutaneously. 4HR was solubilized by 0.1% β-cyclodextrin, and the dosage for 4HR was 10 mg/kg of body weight for 28 days, while the control group received daily injections of the vehicle (0.1% β-cyclodextrin). The initial body weight and tumour size were recorded at the time of the first treatment. The mass size and body weight were recorded every 3 days. The tumour mass size was calculated using the following formula: Mass volume=a (long distance) x b (short distance)<sup>2</sup>/2.

Euthanasia was undertaken when the body weight decreased by 20%, tumour necrosis was observed, or a back hump was observed. The procedure was as follows: mice were deeply anesthetized by 4% isoflurane. Thereafter, mice were quickly sacrificed by cervical dislocation. The death of mice was verified by checking loss of heartbeat.

After the animals were sacrificed, tumour masses were received for histological examination. Briefly, tumour specimens were fixed using 4% formaldehyde diluted by PBS at 4°C for overnight. Paraffin-embedded specimens were cut and prepared for slide. The thickness of cut was 5 μm. Haematoxylin and eosin (H&E) staining was performed for histological examination. The staining procedure was conducted at room temperature and duration was 6 min for haematoxylin and 2 min for eosin. Immunohistochemistry was performed for BCL-2, BAD and BAX, and the same antibodies used for western blotting were used. After hydration, the activity of endogenous peroxidase was blocked by 3% H<sub>2</sub>O<sub>2</sub> at room temperature for 7 min. The protein blocking

was performed using ready-made reagent (cat. no. X0909 Dako; Agilent Technologies, Inc.). After colorization by DAB (cat. no. K5007; Dako Agilent Technologies, Inc.), slides were examined using a light microscope (BX52; Olympus Corporation).

*Statistical analysis.* The data from cell and animal experiments were analysed using Sigma Scan Pro 5.0 and SPSS software ver. 25 (IBM Corp.). The statistical significance of differences between two means was examined using unpaired Student's t-test, whereas multiple values were compared using one-way analysis of variance. P<0.05 was considered to indicate a statistically significant difference. The data were presented as the mean ± standard deviation. The cellular experiments were repeated at least 3 times. Post hoc analysis was completed using Bonferroni comparisons.

## Results

*Conformational change of the peptide from mutant p53 by 4HR administration.* Normal p53 has Glu258, but p53 of YD-15 cells has Ala258. Each peptide has 20 amino acids, including a mutation site. According to amino acid sequence-based peptide conformation prediction, this mutation changes the peptide conformation from a beta-sheet structure to a random coil structure (Fig. 1A) (26,27). The FT-IR spectrum of the peptide showed a series of absorption bands at 1,600-1,700 (amide I), 1,480-1,580 (amide II), and 1,230-1,300 cm<sup>-1</sup> (amide III) (Fig. 1B) (28-30). The amide I

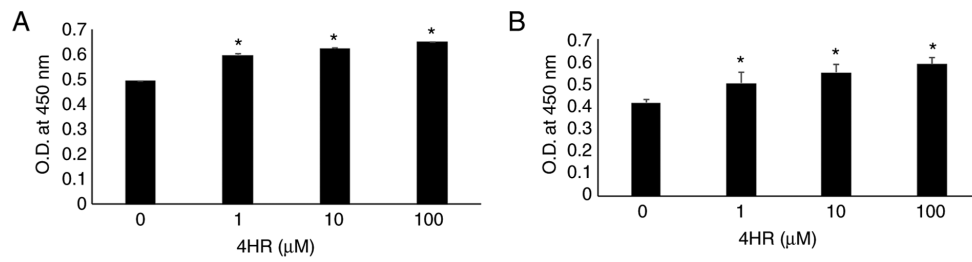


Figure 2. Change in p53 transcriptional activity by 4HR administration. (A) p53 transcriptional activity was significantly increased by 4HR administration in YD-15 cells. (B) p53 transcriptional activity in YD-9 cells. The trend was similar to that of YD-15 cells. \*P<0.05. 4HR, 4-Hexylresorcinol.

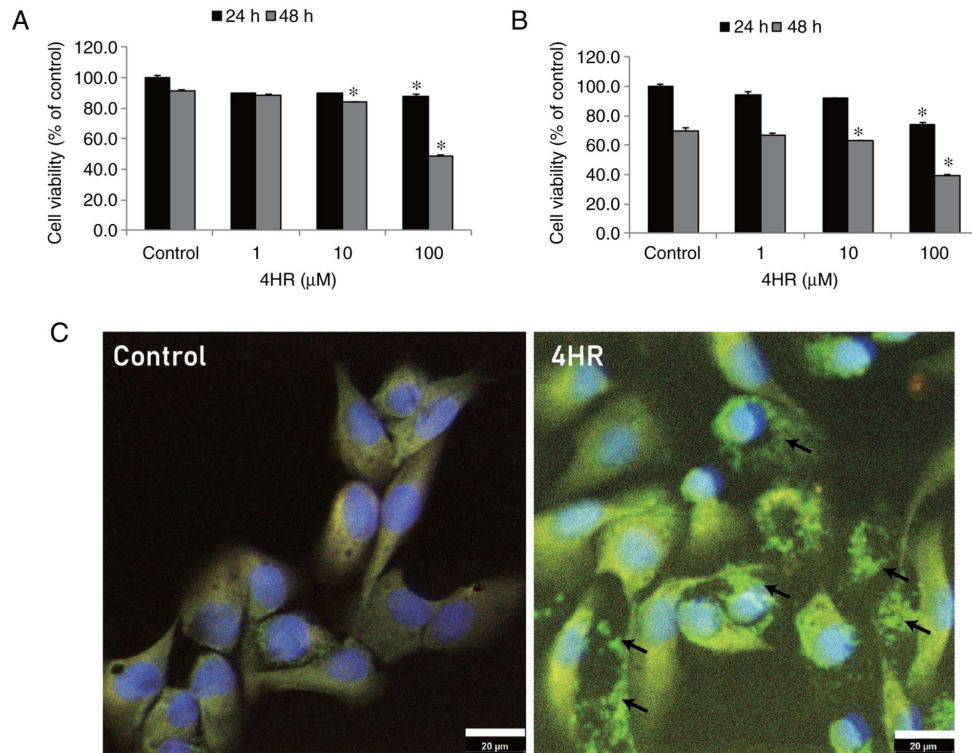


Figure 3. Cellular proliferation and apoptosis by 4HR administration. (A) MTT assay in YD-15 cells. The cellular proliferation of YD-15 cells was suppressed by 4HR administration. (B) MTT assay in YD-9 cells. The trends were similar to those of YD-15 cells. (C) The leakage of cytochrome c from the mitochondria (arrows) was increased by 4HR administration. \*P<0.05. 4HR, 4-Hexylresorcinol.

peak (C=O stretching) position is very sensitive to the conformation types ( $\beta$ -sheet,  $\alpha$ -helix,  $\beta$ -turn, random coil) of the protein secondary structures (28).

Therefore, detailed sub-band assignment of the amide I band is quite useful for evaluating the relative amount of protein secondary structures. In addition to the conventional infrared spectra showing qualitative amounts of protein structures (Fig. 1C), the second derivative spectra of the peptides apparently revealed sub-band peaks assignable to well-known protein secondary structures (Fig. 1D). All examined peptide specimens showed typical vibrational modes corresponding to  $\beta$ -sheet,  $\beta$ -turn and helix structures. One notable conformational change was found; p53 Glu258 showed rich  $\beta$ -sheet conformations detectable at 1,614, 1,628 and 1,639  $\text{cm}^{-1}$ , as indicated in Fig. 1D, whereas p53 Ala258 showed a simple conformation mostly detected at 1628  $\text{cm}^{-1}$ . When p53 Ala-258 was coupled by 4HR, it lost its original conformation and resembled the conformation of p53 Glu-258.

**Increase in p53 transcriptional activity by 4HR administration.** p53 transcriptional activity was significantly increased by 4HR administration (Fig. 2A; P<0.001). The OD value for the untreated control was  $0.494 \pm 0.001$ , and the OD values were  $0.598 \pm 0.007$ ,  $0.622 \pm 0.008$  and  $0.649 \pm 0.002$  for the 1, 10 and 100  $\mu\text{M}$  4HR treatments, respectively. In the post hoc comparison, the difference between the untreated control and 4HR-treated groups was statistically significant (P<0.001). When comparisons between the 4HR-treated groups were conducted, a significant difference was identified (P<0.05). Increased p53-mediated transcriptional activity was also detected in YD-9 cells (Fig. 2B).

**Increase in apoptosis-associated proteins by 4HR administration.** In the MTT assay, the cellular proliferation of YD-15 cells was suppressed by 4HR administration (Fig. 3A). The suppression of tumour cell proliferation by 4HR administration was also observed in YD-9 cells (Fig. 3B). Apoptosis of

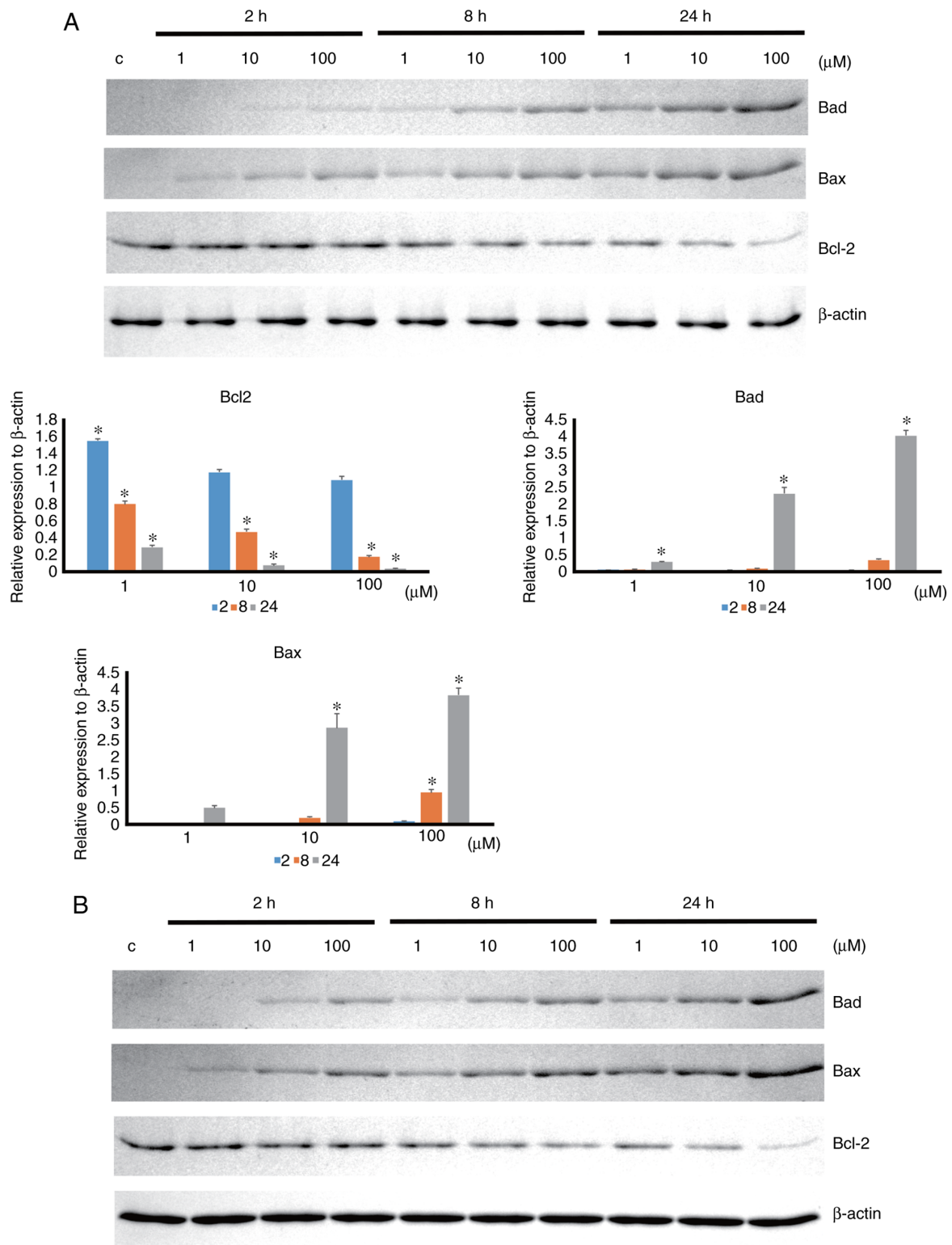


Figure 4. Change in apoptosis-associated protein expression by 4HR administration. (A) The expression of apoptosis-associated proteins in YD-15 cells after 4HR administration. The expression levels of BAD and BAX were increased by 4HR administration in a time- and dose-dependent manner. (B) The expression of apoptosis-associated proteins in YD-9 cells after 4HR administration. \* $P < 0.05$ . 4HR, 4-Hexylresorcinol.

YD-15 cells increased in a dose-dependent manner as revealed by confocal microscopic examination (Fig. 3C).

Apoptosis-associated protein expression was increased by 4HR administration in a time- and dose-dependent manner (Fig. 4). 4HR administration significantly decreased the expression level of BCL-2 anti-apoptotic protein ( $P < 0.001$ ). In

the post hoc comparison, the difference between the untreated control and 4HR-treated groups was statistically significant ( $P < 0.001$  for 100  $\mu$ M 4HR treatment at 2 h and  $P < 0.001$  for all groups at 8 and 24 h). The expression levels of BAD and BAX proapoptotic proteins were significantly increased by 4HR administration ( $P < 0.001$ ). A post hoc comparison was

Table I. Initial tumour size and tumour size at the end of treatment (\*Mice were dead within a week and excluded for plotting in Fig. 5B).

Number	Group	Initial tumour size (mm <sup>3</sup> )	Final tumour size (mm <sup>3</sup> )
1	4HR	86.4	883.2
2	Control	12.4	209.0
4	4HR	49.1	51.4
5	Control	153.3	532.9
6*	Control	40.7	59.7
7	4HR	55.6	158.7
8*	Control	36.8	43.3
9	4HR	4.1	80.7
10*	Control	49.7	82.8
12	Control	39.7	338.4
14	Control	8.3	144.0
15*	4HR	47.7	117.2
16	Control	25.3	170.7
17	Control	25.1	202.1
19	4HR	82.1	49.3
20	4HR	74.4	242.0
	Mean (control)	43.5	198.1
	Mean (4HR)	57.1	226.1

4HR, 4-Hexylresorcinol.

performed for BAD and BAX. The difference in BAD expression between the untreated control and 4HR-treated groups was statistically significant (P=0.003 for 100 µM 4HR treatment at 8 h, P=0.039 for 1 µM 4HR treatment at 24 h, and P<0.001 for 10 and 100 µM 4HR treatment at 24 h). The difference in BAX expression between the untreated control and 4HR-treated groups was statistically significant (P<0.001 for 100 µM 4HR treatment at 8 h and P<0.001 for 10 and 100 µM 4HR treatment at 24 h). A similar pattern of expression was also found in YD-9 cells (Fig. 4B). In the xenograft study, tumours were observed in the sublingual area (Fig. 5A). The 4HR-treated group showed a smaller increase in tumour size than the control group (Fig. 5B, Table I). However, the difference between groups was not significant (P>0.05). Mitosis in the tumour mass was less frequently observed in the 4HR group (Fig. 5C). In the immunohistochemical study, the expression level of BCL-2 was similar between groups (Fig. 5C). However, the expression levels of BAX and BAD were higher in the 4HR group than in the control group (Fig. 5C).

### Discussion

YD-15 cells have a p53 mutation in its DNA binding domain (13). The peptide from the p53 DNA binding domain was prepared from both mutant and normal p53. When 4HR was applied to the mutant peptide, its conformation changed and was close to that of normal p53. The administration of 4HR increased p53 transcriptional activity in both YD-9 and YD-15 cells. The apoptosis induced by 4HR was confirmed by

cytochrome *c* leakage in YD-15 cells after 4HR administration. The expression levels of BAD and BAX were increased by 4HR administration in both YD-9 and YD-15 cells. The expression levels of BAD and BAX in the grafted tumour were increased in the 4HR group compared with the control group. Collectively, 4HR administration to oral cancer cells with a p53 mutation increased p53 transcriptional activity via a potential conformational change in mutant p53 (Fig. 6).

Glutamic acid at the 258th amino acid in p53 was replaced by alanine in YD-15 cells (13). The peptide around the mutant site was designed and synthesized. The conformation of the peptide from mutant p53 was predicted to have a random coil structure, but the conformation of the peptide from normal p53 was a β-sheet structure (26,27). Notably, the administration of p53 changed the conformation of the peptide from mutant p53 and brought it close to that of the peptide from normal p53. This conformational change of mutant p53 by 4HR administration should improve the transcriptional activity of p53. The transcriptional activity of p53 was significantly increased by 4HR administration in both YD-15 and YD-9 cells. Several chemicals have been identified that can change the conformation of mutant p53 (9). However, most of these increase the production of ROS (9). Therefore, while they may be helpful for eliminating tumour cells, they will also induce toxicity in normal organs by systemic administration (31). Compared with previous conformational change chemicals, 4HR has antioxidant activity (32,33). Thus, its systemic application would be relatively safe compared with others (33).

Similar to 4HR, numerous chemicals have been introduced for mutated p53. COTI-2 is a thiosemicarbazone compound. COTI-2 can interact with both full-length mutated p53 and peptide of DNA binding domain from mutated p53 (34). The combination of COTI and cisplatin shows a synergistic effect on head and neck squamous cell carcinoma (35). Notably, the combination of 4HR and cisplatin also shows a synergistic effect on head and neck squamous cell carcinoma (22). When mutated p53 recovers its function, gene transcription and protein expression should be subsequently increased. In healthy cells, the administration of carcinogens activates the p53 signalling pathway in response to DNA damage. BAX is a gene induced by the p53-dependent DNA damage response and results in cytochrome *c* release from the mitochondria (9). BAD is also a proapoptotic protein and is activated by p53 (36). In the present study, administration of 4HR increased the expression levels of BAD and BAX. As a consequence, the release of cytochrome *c* was increased with the inhibition of cellular proliferation.

There are certain limitations to the present study. First, there may have been limitations in the protein conformation study using peptides. Peptides are a partial domain of proteins. If atomic microscopy or X-ray crystallography is used for the study of mutant p53 conformational changes, more detailed information could be acquired. Second, numerous compounds that can recover p53 activity in tumours with p53 mutations have p53-independent effects, and these effects may be beneficial to the treatment of tumours (12). 4HR is an HDAC inhibitor (18). The administration of 4HR decreases the expression level of HDAC4 in HUVECs (18) and Saos-2 cells (37). 4HR is a chemical chaperone (16) that increases the stress of the ER, which may

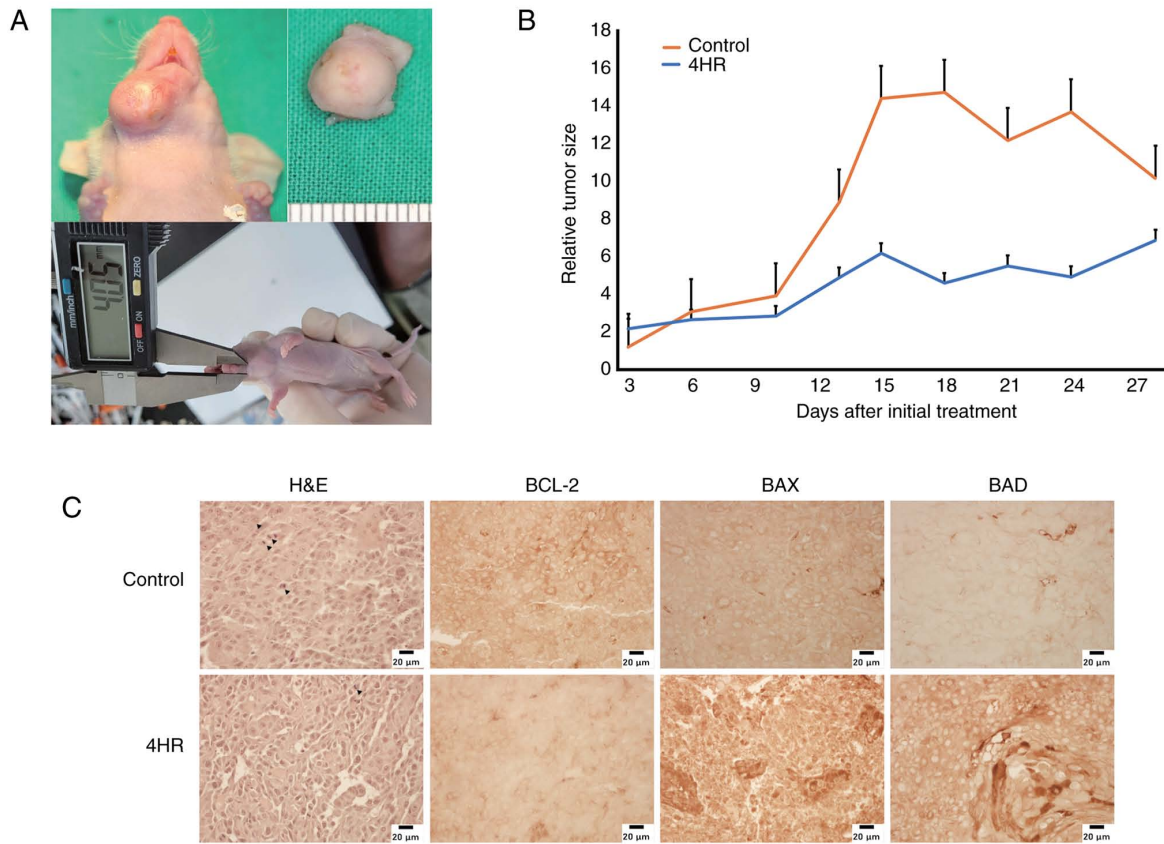


Figure 5. Tumour xenograft study. (A) Grafted tumour mass was observed sublingual area. The size of tumour was measured by an electronic calliper. At the time of euthanasia, tumour specimen was received for the histological analysis. (B) As the mass size at the initial treatment was different among animals, the ratio between the initial mass size and the mass size at each observation was calculated and compared. The relative mass size was higher in the control group than in the 4HR group. However, the difference between groups was not significant. (C) The tumour masses were stained with haematoxylin and eosin. Mitosis (arrowheads) was markedly more frequently observed in the control group. In the immunohistochemical study, the expression level of BCL-2 showed a similar level between groups. However, the expression levels of BAX and BAD were higher in the 4HR group. Images were captured using a light microscope (scale bar, 20  $\mu$ m). 4HR, 4-Hexylresorcinol.

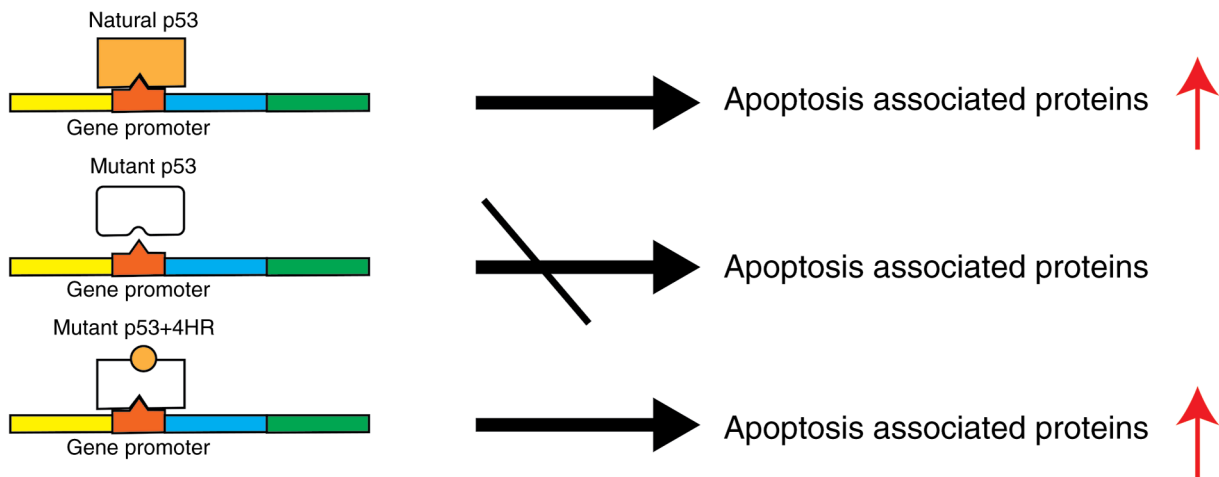


Figure 6. Graphical abstract. As mutant p53 has a mutation in its DNA binding domain, mutant p53 can be expected to have less transcriptional activity. When 4HR is coupled with mutant p53, its DNA binding activity may be increased by its conformational change. As a consequence, p53 transcriptional activity will be recovered. 4HR, 4-Hexylresorcinol.

be induced by changes in protein folding (38). Thus, investigation of acetylation and phosphorylation of p53 would be interesting topic. This will be explored separately in future studies. Third, the YD-15 cell line has been shown to have

poor tumorigenicity in an animal model (13). In the present study, some animals showed successful tumour formation, but their survival rate was poor. Only a few animals survived until the 28th day after the initial treatment, and a

statistically significant difference between groups was not observed. Thus, confirmation of antitumor effects in the animal model was not possible in the current study design. HSC-1, HSC-2 and HSC-4 cells also have mutations in the DNA-binding domain of p53 (39-41). Thus, the study of other types of cancer with mutant p53 will be an interesting topic for future study. In addition, finding essential mutations via gene sequencing was not the objective of the present study. This will also be an interesting research subject for future study. The merit of the current study should be the finding of recovered transcriptional activity of mutant p53 by the administration of 4HR.

In conclusion, 4HR is a potential substance for recovering the loss-of-function in mutant p53 as a chemical chaperone via protein conformational change.

### Acknowledgements

Not applicable.

### Funding

The present study was supported by the 'Cooperative Research Program for Agriculture Science and Technology Development (grant no. PJ01562601)' of the Rural Development Administration of Republic of Korea.

### Availability of data and materials

Data sharing is not applicable to this article, as no datasets were generated or analyzed during the current study.

### Authors' contributions

YJK and SGK conceived and designed the study. DWK and YWG performed the experiments and collected the data. WSC, YJK and SGK analysed and interpreted the data. YJK wrote the paper. SGK and HR reviewed the data and information and edited the manuscript. SGK and HR critically revised the paper for important intellectual content. YJK, WSC and DWK confirm the authenticity of all the raw data. All authors read and approved the final version of the manuscript and agree to be accountable for all aspects of the research in ensuring that the accuracy or integrity of any part of the work are appropriately investigated and resolved.

### Ethics approval and consent to participate

The animal study was approved (approval no. GWN-2021-3; approval date 2021.01.15) by the Animal Care and Use Guidelines of the College of Dentistry at Gangneung-Wonju National University (Gangneung, Republic of Korea).

### Patient consent for publication

Not applicable.

### Competing interests

The authors declare that they have no competing interests.

### References

- Lane DP: Cancer. p53, guardian of the genome. *Nature* 358: 15-16, 1992.
- Levine AJ: p53, the cellular gatekeeper for growth and division. *Cell* 88: 323-331, 1997.
- Xia Z, Kon N, Gu AP, Tavara O and Gu W: Deciphering the acetylation code of p53 in transcription regulation and tumor suppression. *Oncogene* 41: 3039-3050, 2022.
- Pecorino L (ed): *Molecular biology of Cancer*. Oxford University Press, Oxford, 2016.
- Lee JH, Kim HS, Lee SJ and Kim KT: Stabilization and activation of p53 induced by Cdk5 contributes to neuronal cell death. *J Cell Sci* 120: 2259-2271, 2007.
- Brooks CL and Gu W: Ubiquitination, phosphorylation and acetylation: The molecular basis for p53 regulation. *Curr Opin Cell Biol* 15: 164-171, 2003.
- Peltonen JK, Helppi HM, Pääkkö P, Turpeenniemi-Hujanen T and Vähäkangas KH: p53 in head and neck cancer: Functional consequences and environmental implications of TP53 mutations. *Head Neck Oncol* 2: 36, 2010.
- Lindemann A, Takahashi H, Patel A, Osman A and Myers J: Targeting the DNA damage response in OSCC with TP 53 mutations. *J Dent Res* 97: 635-644, 2018.
- de Bakker T, Journe F, Descamps G, Saussez S, Dragan T, Ghanem G, Krayem M and Van Gestel D: Restoring p53 function in head and neck squamous cell carcinoma to improve treatments. *Front Oncol* 11: 799993, 2022.
- Kaida A and Iwakuma T: Regulation of p53 and cancer signaling by heat shock protein 40/J-domain protein family members. *Int J Mol Sci* 22: 13527, 2021.
- Kanapathipillai M: Treating p53 mutant aggregation-associated cancer. *Cancers (Basel)* 10: 154, 2018.
- Muller PA and Vousden KH: Mutant p53 in cancer: New functions and therapeutic opportunities. *Cancer Cell* 25: 304-317, 2014.
- Lee EJ, Kim J, Lee SA, Kim EJ, Chun YC, Ryu MH and Yook JI: Characterization of newly established oral cancer cell lines derived from six squamous cell carcinoma and two mucoepidermoid carcinoma cells. *Exp Mol Med* 37: 379-390, 2005.
- Lambert JM, Gorzov P, Veprintsev DB, Söderqvist M, Segerbäck D, Bergman J, Fersht AR, Hainaut P, Wiman KG and Bykov VJ: PRIMA-1 reactivates mutant p53 by covalent binding to the core domain. *Cancer Cell* 15: 376-388, 2009.
- Chen HM, Lee YH and Wang YJ: ROS-triggered signaling pathways involved in the cytotoxicity and tumor promotion effects of pentachlorophenol and tetrachlorohydroquinone. *Chem Res Toxicol* 28: 339-350, 2015.
- Kim SG: 4-Hexylresorcinol: Pharmacologic chaperone and its application for wound healing. *Maxillofac Plast Reconstr Surg* 44: 5, 2022.
- Lee IS, Chang JH, Kim DW, Kim SG and Kim TW: The effect of 4-hexylresorcinol administration on NAD<sup>+</sup> level and SIRT activity in Saos-2 cells. *Maxillofac Plast Reconstr Surg* 43: 39, 2021.
- Kim JY, Kweon HY, Kim DW, Choi JY and Kim SG: 4-Hexylresorcinol inhibits class I histone deacetylases in human umbilical cord endothelial cells. *Appl Sci* 11: 3486, 2021.
- Kim DW, Jo YY, Garagiola U, Choi JY, Kang YJ, Oh JH and Kim SG: Increased level of vascular endothelial growth factors by 4-hexylresorcinol is mediated by transforming growth factor-β1 and accelerates capillary regeneration in the burns in diabetic animals. *Int J Mol Sci* 21: 3473, 2020.
- Jiménez-Urbe AP, Gómez-Sierra T, Aparicio-Trejo OE, Orozco-Ibarra M and Pedraza-Chaverri J: Backstage players of fibrosis: NOX4, mTOR, HDAC, and SIP; companions of TGF-β. *Cell Signal* 87: 110123, 2021.
- Kim SG, Jeon GJ, Park YW, Song JY, Kim AS, Choi JY and Chae WS: 4-Hexylresorcinol inhibits transglutaminase-2 activity and has synergistic effects along with cisplatin in KB cells. *Oncol Rep* 25: 1597-1602, 2011.
- Kim SG, Lee SW, Park YW, Jeong JH and Choi JY: 4-hexylresorcinol inhibits NF-κB phosphorylation and has a synergistic effect with cisplatin in KB cells. *Oncol Rep* 26: 1527-1532, 2011.
- Xue L, Zhou B, Liu X, Qiu W, Jin Z and Yen Y: Wild-type p53 regulates human ribonucleotide reductase by protein-protein interaction with p53R2 as well as hRRM2 subunits. *Cancer Res* 63: 980-986, 2003.

24. Luo J, Su F, Chen D, Shiloh A and Gu W: Deacetylation of p53 modulates its effect on cell growth and apoptosis. *Nature* 408: 377-381, 2000.
25. Zhang Y, Dong Y, Wu X, Lu Y, Xu Z, Knapp A, Yue Y, Xu T and Xie Z: The mitochondrial pathway of anesthetic isoflurane-induced apoptosis. *J Biol Chem* 285: 4025-4037, 2010.
26. Shen Y, Maupetit J, Derreumaux P and Tufféry P: Improved PEP-FOLD approach for peptide and miniprotein structure prediction. *J Chem Theory Comput* 10: 4745-4758, 2014.
27. Thévenet P, Shen Y, Maupetit J, Guyon F, Derreumaux P and Tufféry P: PEP-FOLD: An updated de novo structure prediction server for both linear and disulfide bonded cyclic peptides. *Nucleic Acids Res* 40 (Web Server Issue): W288-W293, 2012.
28. Kong J and Yu S: Fourier transform infrared spectroscopic analysis of protein secondary structures. *Acta Biochim Biophys Sin (Shanghai)* 39: 549-559, 2007.
29. Jo YY, Kweon H, Kim DW, Baek K, Kim MK, Kim SG, Chae WS, Choi JY and Rotaru H: Bone regeneration is associated with the concentration of tumour necrosis factor- $\alpha$  induced by sericin released from a silk mat. *Sci Rep* 7: 15589, 2017.
30. Jo YY, Kweon H, Kim DW, Baek K, Chae WS, Kang YJ, Oh JH, Kim SG and Garagiola U: Silk sericin application increases bone morphogenic protein-2/4 expression via a toll-like receptor-mediated pathway. *Int J Biol Macromol* 190: 607-617, 2021.
31. Buonocore G, Perrone S and Tataranno ML: Oxygen toxicity: Chemistry and biology of reactive oxygen species. *Int J Biol Macromol* 15: 186-190, 2010.
32. Yen GC, Duh PD and Lin CW: Effects of resveratrol and 4-hexylresorcinol on hydrogen peroxide-induced oxidative DNA damage in human lymphocytes. *Free Radic Res* 37: 509-514, 2003.
33. Guandalini E, Ioppolo A, Mantovani A, Stacchini P and Giovannini C: 4-Hexylresorcinol as inhibitor of shrimp melanosis: Efficacy and residues studies; evaluation of possible toxic effect in a human intestinal in vitro model (Caco-2); preliminary safety assessment. *Food Addit Contam* 15: 171-180, 1998.
34. Synnott NC, O'Connell D, Crown J and Duffy MJ: COTI-2 reactivates mutant p53 and inhibits growth of triple-negative breast cancer cells. *Breast Cancer Res Treat* 179: 47-56, 2020.
35. Lindemann A, Patel AA, Silver NL, Tang L, Liu Z, Wang L, Tanaka N, Rao X, Takahashi H, Maduka NK, *et al*: COTI-2, a novel thiosemicarbazone derivative, exhibits antitumor activity in HNSCC through p53-dependent and-independent mechanisms. *Clin Cancer Res* 25: 5650-5662, 2019.
36. Gao L, Yu L, Li CM, Li Y, Jia BL and Zhang B: Karyopherin  $\alpha$ 2 induces apoptosis in tongue squamous cell carcinoma CAL-27 cells through the p53 pathway. *Oncol Rep* 35: 3357-3362, 2016.
37. Lee IS, Kim DW, Oh JH, Lee SK, Choi JY, Kim SG and Kim TW: Effects of 4-hexylresorcinol on craniofacial growth in rats. *Int J Mol Sci* 22: 8935, 2021.
38. Kim JY, Kim DW, Lee SK, Choi JY, Che X, Kim SG and Garagiola U: Increased expression of TGF- $\beta$ 1 by 4-hexylresorcinol is mediated by endoplasmic reticulum and mitochondrial stress in human umbilical endothelial vein cells. *Appl Sci* 11: 9128, 2021.
39. Hori M, Suzuki K, Udono MU, Yamauchi M, Mine M, Watanabe M, Kondo S and Hozumi Y: Establishment of ponasterone A-inducible the wild-type p53 protein-expressing clones from HSC-1 cells, cell growth suppression by p53 expression and the suppression mechanism. *Arch Dermatol Res* 301: 631-646, 2009.
40. Kashiwazaki H: Detectability and diagnostic criteria of p53 gene mutations in human oral squamous cell carcinoma using yeast functional assay. *Hokkaido Igaku Zasshi* 72: 211-224, 1997 (In Japanese).
41. Ichwan SJ, Yamada S, Sumrejkanchanakij P, Ibrahim-Auerkari E, Eto K and Ikeda MA: Defect in serine 46 phosphorylation of p53 contributes to acquisition of p53 resistance in oral squamous cell carcinoma cells. *Oncogene* 25: 1216-1224, 2006.



This work is licensed under a Creative Commons Attribution-NonCommercial-NoDerivatives 4.0 International (CC BY-NC-ND 4.0) License.